Veterinary Parasitology 196 (2013) 409–416

Contents lists available at SciVerse ScienceDirect

Veterinary Parasitology

journal homepage: www.elsevier.com/locate/vetpar

Comparative analysis of *Trichuris muris* surface using conventional, low vacuum, environmental and field emission scanning electron microscopy

Eduardo José Lopes Torres[a,b,c], Wanderley de Souza[b,c,d], Kildare Miranda[b,d,*]

[a] *Laboratório de Helmintologia Roberto Lascasas Porto, Departamento de Microbiologia, Imunologia e Parasitologia, Faculdade de Ciências Médicas, Universidade do Estado do Rio de Janeiro, Av. Professor Manoel de Abreu 444/5° andar, Vila Isabel, Rio de Janeiro CEP 20511-070, RJ, Brazil*

[b] *Laboratório de Ultraestrutura Celular Hertha Meyer, Instituto de Biofísica Carlos Chagas Filho and Instituto Nacional de Ciência e Tecnologia em Biologia Estrutural e Bioimagens, Universidade Federal do Rio de Janeiro, Av. Carlos Chagas Filho, 373, Bloco G subsolo, Cidade Universitária, Ilha do Fundão, Rio de Janeiro 21941-902, RJ, Brazil*

[c] *Laboratório de Biologia de Helmintos Otto Wucherer, Programa de Biologia Celular e Parasitologia, Instituto de Biofísica Carlos Chagas Filho, Universidade Federal do Rio de Janeiro, Av. Carlos Chagas Filho, 373, Bloco I, 2° andar, sala 35, Cidade Universitária, Ilha do Fundão, Rio de Janeiro CEP 21949-902, RJ, Brazil*

[d] *Diretoria de Programas, Instituto Nacional de Metrologia, Qualidade e Tecnologia (Inmetro), Xerém, Duque de Caxias, RJ, Brazil*

ARTICLE INFO

Article history:
Received 17 December 2012
Received in revised form 4 February 2013
Accepted 26 February 2013

Keywords:
Helminth
Nematode
Cuticle
Bacillary band
Host–parasite interactions
Intestine

ABSTRACT

The whipworm of the genus *Trichuris* Roederer, 1791, is a nematode of worldwide distribution and comprises species that parasitize humans and other mammals. Infections caused by *Trichuris* spp. in mammals can lead to various intestinal diseases of human and veterinary interest. The morphology of *Trichuris* spp. and other helminths has been mostly studied using conventional scanning electron microscopy of chemically fixed, dried and metal-coated specimens, although this kind of preparation has been shown to introduce a variety of artifacts such as sample shrinking, loss of secreted products and/or hiding of small structures due to sample coating. Low vacuum (LVSEM) and environmental scanning electron microscopy (ESEM) have been applied to a variety of insulator samples, also used in the visualization of hydrated and/or live specimens in their native state. In the present work, we used LVSEM and ESEM to analyze the surface of *T. muris* and analyze its interaction with the host tissue using freshly fixed or unfixed hydrated samples. Analysis of hydrated samples showed a set of new features on the surface of the parasite and the host tissue, including the presence of the secretory products of the bacillary glands on the surface of the parasite, and the presence of mucous material and eggs on the intestinal surface. Field emission scanning electron microscopy (FESEM) was also applied to reveal the detailed structure of the glandular chambers in fixed, dried and metal coated samples. Taken together, the results show that analysis of hydrated samples may provide new insights in the structural organization of the surface of helminth parasites and its interaction with the infected tissue, suggesting that the application of alternative SEM techniques may open new perspectives for analysis in taxonomy, morphology and host–parasite interaction fields.

* Corresponding author at: Laboratório de Ultraestrutura Celular Hertha Meyer, Instituto de Biofísica Carlos Chagas Filho and Instituto Nacional de Ciência e Tecnologia em Biologia Estrutural e Bioimagens, Universidade Federal do Rio de Janeiro, Av. Carlos Chagas Filho, 373, Bloco G subsolo, Cidade Universitária, Ilha do Fundão, Rio de Janeiro 21941-902, RJ, Brazil. Tel.: +55 21 22602364; fax: +55 21 22602364.
E-mail addresses: kmiranda@biof.ufrj.br, kildare.miranda@gmail.com (K. Miranda).

0304-4017/$ – see front matter © 2013 Elsevier B.V. All rights reserved.
http://dx.doi.org/10.1016/j.vetpar.2013.02.026

1. Introduction

Tissue-dwelling intestinal nematodes are spread throughout the world. It is estimated that these parasites currently infect over two billion people, causing morbidity and debility in infected individuals, especially in developing countries, being a food safety and health problem worldwide (Patel et al., 2009). Among the nematodes of high interest with respect to the mechanisms of interaction with the host tissue are the hookworms, which interact with their hosts by inserting cuticular teeth in the intestinal epithelium, and the whipworms, which during infection create an intra-tissue niche in the cells of the large intestine (Hall et al., 2008). Whipworms of the genus *Trichuris* have global distribution and comprise nematode species that parasitize humans and other mammals (Cafrune et al., 1999). Among these parasites, *Trichuris muris* has been used as a model in parasite–mouse epithelial tissue interaction studies. Alterations of the epithelial surface induced by the presence of these nematodes have been extensively characterized using different microscopy techniques, where the surface analysis of nematodes (especially in regions where it interacts with the host cells) and of the host tissue (in host–pathogen interaction) has been carried out mainly using scanning electron microscopy (SEM) as a tool (Wright, 1975; Batte et al., 1977; Tilney et al., 2005).

Identification of nematode species is usually carried out using light microscopy, although SEM analysis has also been used as a complementary tool. More recently, a combined taxonomical approach, where analysis of morphological characteristics by different microscopy methods is complemented by sequence analysis with different molecular biology tools, has led to important steps towards the consolidation of integrated taxonomical studies in the field of helminthology (Knoff et al., 2012). Nevertheless, it is worth mentioning that conventional SEM analysis remains one of the most popular tools for the structural characterization of the surface of *Trichuris*, considered to contain relevant structures for both taxonomical characterization (*e.g.*, the vulvar region, the spicule prepuce and the bacillary band) and host–parasite interaction studies (Wright, 1975; Gomes et al., 1992; Tenora et al., 1993; Lanfredi et al., 1995; Robles and Navone, 2006).

Despite the wide application of SEM in the structural characterization of biological surfaces, it has been extensively shown in different models that sample preparation and imaging strategies used in traditional approaches can introduce artifacts that may potentially change the sample surface, leading to the imprecise interpretation of the morphological data. These include sample shrinking, leaching of material, and loss of small structures, which can also be hidden after the formation of relatively thick metal coating (Muscariello et al., 2005). In the case of nematodes and the host tissue, several structures may be potentially modified, lost or hidden, including the products secreted by the parasite and the mucous secreted by the host goblet cells. In addition, small adult worms and eggs may be lost in the washing, dehydration and/or the critical-point drying steps.

Developments in SEM technology over the past 30 years have gone far to overcome some of the constraints on SEM operation and sample preparation. One major advance was the development of scanning electron microscopes that operate under low vacuum, allowing the visualization and analysis of non conductive, uncoated or hydrated samples (Shah and Beckett, 1979; Danilatos, 1981, 1988). Two main types of instruments, so-called variable pressure SEMs, are available: the low vacuum SEM (which here will be referred to as LVSEM) that operates with a working pressure of ~115–130 Pa in the chamber, and the environmental SEM (ESEM) that operates with a working pressure of ~390–500 Pa and usually requires the use of a Peltier sample cooling system.

In this work, we report the use of conventional SEM (CSEM) for analysis of fixed, dried and coated samples; LVSEM, for the analysis of fixed and hydrated samples; and ESEM for the analysis of unfixed samples. Field emission scanning electron microscopy (FESEM) was also applied to reveal the detailed structure of the glandular chambers in critical-point dried and metal coated samples.

Analyses of chemically fixed and critical-point dried samples showed that the secretory products of the bacillary gland openings were extracted, whereas when wet samples (fixed and unfixed) were analyzed using both LVSEM and ESEM, the glandular products were better preserved and could be seen in each glandular opening in all glands analyzed. In addition, when the infected intestinal tissue was analyzed under hydrated conditions (fixed), mucous material and large structures such as eggs were observed on the intestinal surface, in contrast to conventionally prepared samples. Altogether, these results suggest that LVSEM and ESEM can be used as tools for improved analysis of hydrated (fixed or unfixed) helminth samples. CSEM is a consolidated technique to study the biology of helminthes. The possibility of analyzing hydrated samples can, nevertheless, open new perspectives in taxonomy, morphology and host–parasite interaction.

2. Materials and methods

2.1. Ethics statement

The parasite life cycle was maintained in the Otto Wucherer Helminth Biology Laboratory and all animal protocols were approved by the Ethics Committee for Animal Experimentation of the Health Sciences Center of Federal University of Rio de Janeiro, under the Protocol IBCCF 149, according to Brazilian federal law (Law 11,794/2008, regulated by Decree 6,899/2009), based on the "Guide for the Care and Use of Laboratory Animals" prepared by the National Academy of Sciences, USA, and the "Australian Code of Practice for Care and Use of Animal for Scientific Purpose." All animals received humane care in compliance with the above-mentioned guides used by the Ethics Committee to approve the protocol.

2.2. Experimental infection

Eggs from the *T. muris* Edinburgh strain were provided by Dr. Francisco Bolas (Universidad Complutense de

Madrid), were washed twice in dechlorinated water and incubated at 28 ± 2 °C for 45 days. Ten μL aliquots were mounted and the percentage of embryonated eggs was estimated by light microscopy. Two hundred embryonated eggs, in 0.3 mL of dechlorinated water, were administered orally to ten laboratory-bred Swiss mice aged 4–6 weeks. Imunomodulation was carried out with 50 μL of dexamethasone sodium phosphate (8 mg/mL) and dexamethasone acetate (10 mg/mL) after seven, nine and eleven days post-infection. After 45 days of infection, the mice were euthanized (in a CO_2 chamber), necropsied and the infected tissue of the large intestine (cecum) was recovered. The average infection was around 80 worms/infected mice. All experiments described in this work were performed on samples of the cecum tissue of Swiss mice infected with *T. muris*.

2.3. Conventional scanning electron microscopy (CSEM)

Three fragments of the infected cecum from different mice and 20 nematodes were gently removed with the aid of a round brush (#4) and immediately transferred to a tube containing a fixative solution that consisted of 2.5% glutaraldehyde; 4% freshly prepared formaldehyde in 0.1 M cacodylate buffer, pH 7.2. Samples were fixed for 1 h at room temperature and 12 h at 4 °C. Samples were then subsequently washed in 0.1 M cacodylate buffer, pH 7.2; post-fixed in 1% OsO_4 and 0.8% $K_3Fe(CN)_6$; washed in 0.1 M cacodylate buffer, pH 7.2; dehydrated in a graded ethanol series (20–100° GL) for one hour each step; critical-point dried in CO_2; mounted on metallic stubs and coated with gold (20–25 nm deposited). The samples were examined under Jeol JSM-5310 and FEI Quanta 250 scanning electron microscopes, both operating at 25–30 kV and a pressure of $2–8 \times 10^{-4}$ Pa.

2.4. Field-emission scanning electron microscopy (FESEM)

Ten nematodes were prepared as for the CSEM. The thickness of the gold coat was 3–5 nm Samples were analyzed using a Jeol JSM-6340F microscope, operating at 5 kV

2.5. Low vacuum scanning electron microscopy (LVSEM)

Nematodes (approx. 50 specimens) and three infected tissues from different mice were fixed as for the CSEM, washed in 0.1 M cacodylate buffer, pH 7.2, and mounted on metallic stubs with conductive liquid silver paint (PELCO®) and immediately observed under an FEI Quanta 250 LVSEM operating at 25–30 kV and pressure of 115–130 Pa

2.6. Environmental scanning electron microscopy (ESEM)

Nematodes (approx. 70 specimens) and four infected tissues from different mice were quickly washed in pure water and mounted on concave metallic stubs and directly observed under a Quanta 250 SEM operating at 25 kV, with pressure controlled by water vapor of 390–500 Pa, at 5 °C and humidity of 80–100%.

3. Results

3.1. Structural organization of the surface of the bacillary band

Observation of nematodes using CSEM, LVSEM and ESEM showed a characteristic bacillary band in the cuticular surface of *T. muris*. This was restricted to the anterior region of the ventrolateral face, a characteristic feature of the *Trichuris* genus. This structure, however, presented a different morphological aspect depending on the sample preparation method applied and imaging condition used. CSEM analysis of the cuticle surface (on dried samples) showed cuticular inflations bordering part of the bacillary gland region (Fig. 1A), and the bacillary gland openings as pores (Fig. 1B). When fixed/hydrated samples were analyzed using the LVSEM, collapsed cuticular inflations were observed (Fig. 1C and D). Hydrated unfixed samples (in close-to-native conditions) observed in the ESEM showed a turgid aspect running along the extension of the anterior region of the parasite (Fig. 1E). Nevertheless, cuticular inflations in these preparations presented a collapsed aspect (Fig. 1F).

In contrast to other nematodes, the anterior region of the cuticle of Trichocephalida nematodes presents a bacillary band, a specialized region that contains several glands (bacillary glands) and cuticular pores associated with their openings. When CSEM was used to analyze chemically fixed and dried parasites, these openings were observed as pores without a secretory product (Fig. 2A), although a few pores containing the secretory product could eventually be seen (Fig. 2A inset). Folding of the cuticle surface was also observed in the whole extension of the bacillary band (Fig. 2A, inset). In fixed/hydrated samples analyzed at higher magnification using the low vacuum mode, shrinking of portions of the nematode body was observed, although all bacillary gland openings were filled with an amorphous material and presented a projected pattern (Fig. 2B, inset). Unfixed nematodes analyzed in the ESEM did not present a characteristic shrinking (Fig. 1E) when compared to fixed samples analyzed under low vacuum, and showed a similar overall shape when compared to critical-point dried samples prepared for CSEM. In the environmental mode, it was also possible to identify the amorphous material (presumably the secretory products) projecting from the glandular openings (Figs. 1E and 2C). A detailed observation of the glandular openings in chemically fixed, dried and coated samples by FESEM showed that globular structures organized in clusters were present inside the bacillary gland chambers (Fig. 2D). Although chemical fixation and the subsequent steps for conventional sample preparation for SEM were used, the partial extraction of the amorphous material (previously seen both by LVSEM and ESEM) favored the visualization of structures located within the gland cavity (underneath the amorphous material).

3.2. Interaction of Trichuris muris with cecum of the host

CSEM analysis of the infected tissue (in critical-point dried samples) showed the anterior region of the

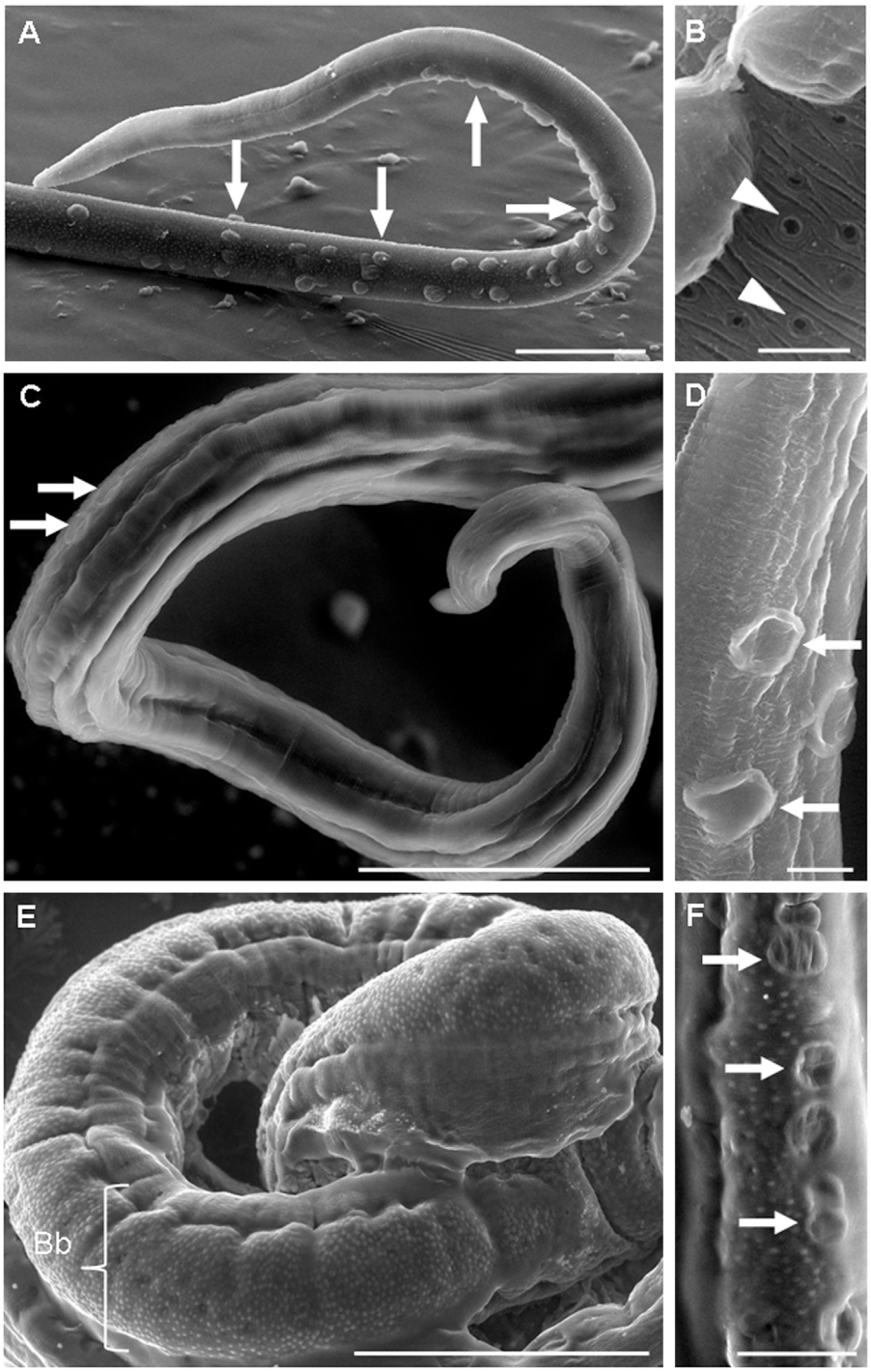

Fig. 1. Adult specimens of *Trichuris muris*: (A) CSEM of the anterior region showing the bacillary band (arrows) on the ventrolateral surface. (B) Cuticular inflation and the bacillary gland openings presenting a pore-shaped structure (arrowhead). (C) LVSEM of the anterior region of the parasite body showing the bacillary band with collapsed cuticular inflations (arrows). (D) Detail of the cuticular surface and collapsed cuticular inflations (arrows). (E) ESEM of the anterior region, showing the bacillary band with bacillary glands presenting a prominent pattern. Bb, Bacillary band. (F) Collapsed cuticular inflations (arrows) and bacillary gland openings. Scale bars: A: 100 μm, B: 10 μm, C: 100 μm, D: 10 μm, E: 100 μm and F: 30 μm.

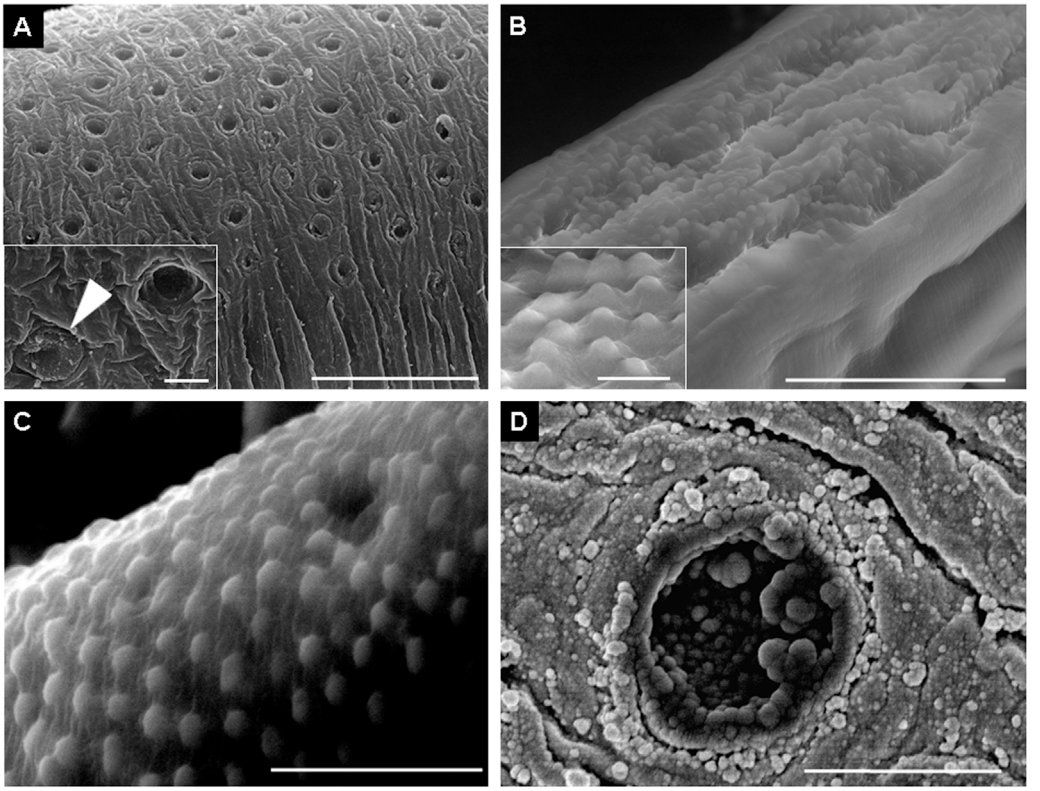

Fig. 2. Bacillary band of adult specimens of *Trichuris muris*: (A) CSEM of the surface of the bacillary band, showing the bacillary gland pores, Inset: Detail of two bacillary gland openings, one filled (arrowhead) with a glandular content and the other as a pore-like structure. (B) LVSEM of the ventro-lateral surface showing the bacillary band with bacillary glands, inset: Detail of the bacillary gland opening presenting a projected pattern. (C) ESEM of the bacillary glands presenting a prominent pattern. (D) FESEM of the bacillary gland, showing the chamber filled with globular structures. Scale bars: A: 10 μm, inset 1 μm, B: 30 μm, inset 5 μm, C: 10 μm and and D: 1 μm.

nematodes inserted in the epithelium of the host intestine and a free posterior region (beginning in the parasite docking site) in the lumen proper. A projection of the epithelial cells towards the intestinal lumen was observed in the regions where the parasite was present (Fig. 3A). The crypts of Lieberkuhn presented a honeycomb aspect (Fig. 3A and B) and the surface of the mucosa that covered the nematode showed blister-like deformations (Fig. 3B).

In contrast to samples submitted to CSEM (both preparation and observation conditions), analysis of fixed/hydrated infected tissues by LVSEM showed a large amount of mucous material on the surface of the epithelium. The posterior region of the parasite body, previously seen as a free region in CSEM, appeared as a partially embedded structure in the mucous layer (Fig. 3C). The presence of prominent quantities of mucous was especially found in epithelium folds (Fig. 3D). In addition, this approach allowed the observation of the eggs on the epithelium surface, rarely seen when CSEM prepared samples are analyzed. Crypts of Lieberkuhn and goblet cell pores were also observed in this sample, suggesting that this approach may provide a better preservation of the tissue (Fig. 3E and F).

Unfixed infected intestinal tissue was also observed using the environmental mode. Analyses of freshly collected material showed nematodes inserted in the intestinal tissue, as before, but totally covered with mucous material. Blister-like deformations were eventually seen on the tissue surface (Fig. 3G). Nevertheless, observation of turgid cells on the intestinal tissue surface was more pronounced in ESEM analysis, suggesting a solid compromise between resolution and sample preservation (Fig. 3H).

4. Discussion

The structure of the surface of nematodes of the *Trichuris* genus has been widely explored by means of different microscopy techniques (Sheffield, 1963; Wright, 1968, 1975; Jenkins, 1969; Wright and Chan, 1973; Batte et al., 1977; Tilney et al., 2005). In the case of scanning electron microscopy, the topographic characterization of the cuticular surface of *T. vulpis*, *T. myocastoris*, *T. suis* and *T. muris* has been performed essentially in critical-point dried samples analyzed under high vacuum (Wright, 1975; Batte et al., 1977; Tilney et al., 2005). Here, we analyzed the surface of *T. muris* and the infected host tissue by means of a collection of SEM modalities (as well as sample preparation conditions) and compared the efficiency of each method in the identification of surface characteristics of the parasite and the host tissue.

In general, a specific combination of sample preparation techniques and imaging conditions resulted in an

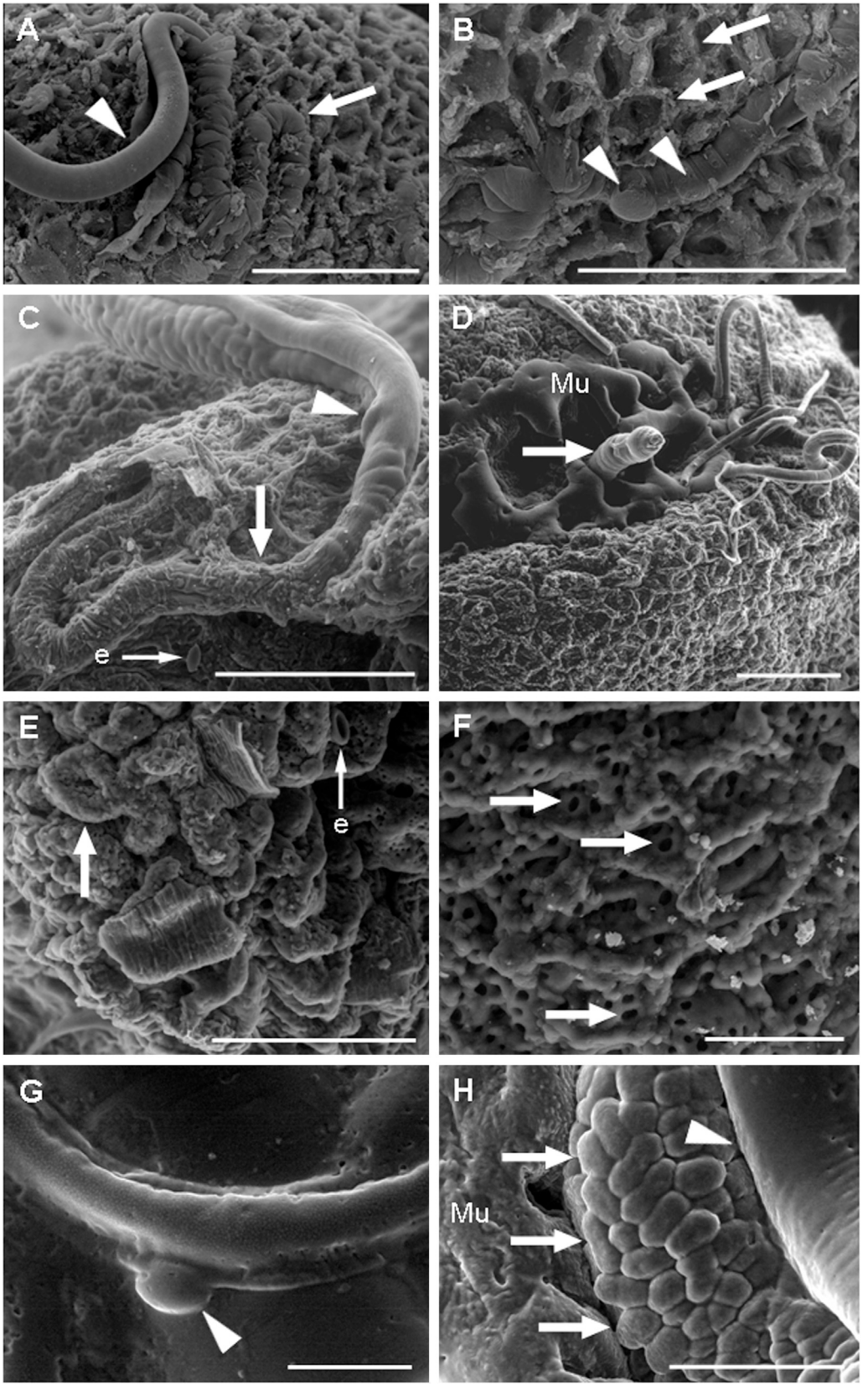
A
B
C
e
D
Mu
E
e
F
G
H
Mu

improved preservation of the sample characteristics, differing to a lower or higher extent from the previous information generated from critical-point dried samples. For instance, previous characterization of live or fixed (critical-point dried) nematodes by light and scanning electron microscopy, respectively, have suggested that the cuticular inflations present in the cuticular surface of the parasites may present semi-spherical (Batte et al., 1977), crater-like or sucker-like organization patterns (Wright, 1975; Zaman, 1984). Our results showed that depending on the sample preparation and imaging condition, this structure may present a turgid aspect (semi-spherical pattern) or crater-like morphology. Nematodes gently removed, freshly fixed, and critical point dried following a fine control in the substitution conditions were shown to contain semi-spherical cuticular inflations. However, it is not uncommon to find cuticular inflations with a crater-like morphology in critical point dried samples, since, depending on the experimental conditions, preparations may present critical point drying artifacts. As samples observed using the LVSEM (of fixed hydrated samples) and ESEM (of unfixed samples), presented a crater-like morphology, we believe that this is a result of a compromise between the benefits of imaging hydrated samples and the dehydration that occurs during imaging due to the microscope residual vacuum. In this regard, the massive shrinkage of the parasite body seen when fixed nematodes were observed under low vacuum, suggest that this imaging condition is more adequate for the analysis of dried, uncoated samples. Imaging of unfixed samples in the environmental mode, on the other hand, did not show any perceptible overall body shrinkage during the initial steps of image acquisition (images generally revealed a turgid aspect of the nematode body), although more sensitive structures such as the cuticular inflations presented a collapsed aspect. Nevertheless, in such conditions the parasites presented an overall improved preservation that can be attributed mainly to the fine control of the temperature and humidity within the microscope chamber.

Another interesting observation was the organization of the glandular openings in nematodes submitted to each method. Previous studies have suggested that the openings of the bacillary glands exist as empty pores spread over the entire surface of the bacillary band (Sheffield, 1963; Wright, 1968, 1975; Jenkins, 1969; Wright and Chan, 1973; Batte et al., 1977; Tilney et al., 2005), although the presence of small circular elevated bodies in glandular openings has also been suggested (Zaman, 1984). Here, CSEM analysis showed that most of the bacillary gland openings presented empty chambers (pore phenotype) and the projected pattern was less frequently seen. Analysis at low vacuum and environmental mode showed that all glandular openings presented a projected pattern, suggesting that the secretion products may have been washed out during sample preparation steps used in CSEM. Although we believe that the successive steps of dehydration and critical point drying are the main cause of extraction, as we inferred preservation by evaluating empty or filled patterns, we cannot rule out the possibility of a mild extraction during chemical fixation. Considering that this is a nematode that interacts with the host intestine and that these products mediate this interaction, being essential to modulate the host's immune system, it is important to have tools that allow the observation of such structures in a close-to-the-native state, so that the secretion products can be imaged and the activity of the glands evaluated *in situ*. Nevertheless, despite the clear disadvantage of removing secretion products during sample preparation for CSEM, analysis of "empty" glands at higher resolution by FESEM showed globular structures inside the bacillary gland chamber, supporting our previous observation in the bacillary glands of *T. thrichomysi* (Lopes Torres et al., 2010). This suggests that the structural characterization of the glands may be more efficient when combined SEM approaches are used.

The semi-rigid cuticle that covers the entire body and the initial and terminal part of the digestive tube provides surface stability and resistance to topographic studies under environmental conditions. As the cuticular surface is the site where all taxonomic characteristics are found, SEM analysis of hydrated samples may potentially generate additional information that, when combined with molecular biology data, may provide grounds for the establishment of integrated taxonomical studies.

From the host point of view, it has been described that the presence of the parasite induces a series of lesions on the surface of the intestinal epithelium, which can be easily seen in different samples prepared for CSEM (Batte et al., 1977; Tilney et al., 2005), and modulates the physiological activity of the host tissue. In this regard, it is known that different parasites induce the production of mucous by goblet cells present in the intestine, although the structural correlation with functional and physiological data has not been achieved with CSEM analysis. Here we showed that this is mainly due to the extraction of the mucous content during sample preparation, since LVSEM and ESEM analysis of freshly collected fixed or unfixed intestines shows a considerable amount of mucous that both protects the epithelial surface and interacts with the parasite surface.

Taken together, our results show the importance of studying the nematode surfaces and their parasitic niches by different SEM techniques, mainly using preparation methods that enable analysis of hydrated samples. Each

Fig. 3. Cecum of Swiss mice infected with *Trichuris muris*: (A) CSEM of the anterior region of the nematode covered with wrinkled cecal mucosa (arrow) and posterior region in the lumen of the cecum (arrowhead). (B) The mucosal surface showing the crypts of Lieberkuhn (arrows) and the blister-like deformations in the region where the nematode is covered by the epithelium (arrowhead). (C) LVSEM of the anterior region of the nematode embedded in a wrinkled cecal mucosa and mucous (arrow), posterior region of the lumen of the cecum (arrowhead) and of the mucosal surface showing eggs (e). (D) Nematodes inserted in one mucosal fold (arrow), showing more mucous (Mu). (E) The mucosal surface showing the crypts of Lieberkuhn (arrow) and collapsed egg (e). (F) Detail of the mucosa surface, showing goblet cell pores (arrows). (G) ESEM of the anterior region of the nematode embedded in the cecal mucosa with a blister-like deformation on the mucosa surface (arrowhead). (H) Mucosa surface covered with mucous (Mu), showing turgid cells (arrows) and deformation that may have been caused by the presence of *T. muris* (arrowhead). Scale bars: A–D: 500 μm; E: 300 μm; F: 100 μm; G–H: 100 μm.

technique is complementary to the other, and a multi-technique approach may provide a better visualization of live nematodes and their interaction with their hosts.

Acknowledgments

We are grateful to Dr. Rovilson Gilioli of CEMIB-UNICAMP, Dr. Arnaldo Maldonado Jr. of FIOCRUZ-IOC and Dr. Francisco Bolas Fernandez of Universidad Complutense de Madrid. This work was supported by grants to the authors from the following Brazilian agencies: Conselho Nacional de Desenvolvimento Científico e Tecnológico (CNPq), Programa Jovens Pesquisadores CNPq, Financiadora de Estudos e Projetos (FINEP) and, the Fundação Carlos Chagas Filho de Amparo à Pesquisa do Estado do Rio de Janeiro (FAPERJ).

References

Batte, E.G., Mclamb, R.D., Muse, K.E., Tally, S.D., Vestal, T.J., 1977. Pathophysiology of swine trichuriasis. Am. J. Vet. Res. 38, 1075–1079.

Cafrune, M.M., Aguirre, D.H., Rickard, L.G., 1999. Recovery of *Trichuris tenuis* Chandler, 1930, from camelids (*Lama glama* and *Vicugna vicugna*) in Argentina. J. Parasitol. 85, 961–962.

Danilatos, G.D., 1981. Design and construction of an atmospheric of environmental SEM. Scanning 4, 9–20.

Danilatos, G.D., 1988. Foundations of environmental scanning electron microscopy. In: Hawkes, P.W. (Ed.), Advances in Electronics and Electron Physics, vol. 71. Academic Press, Boston, pp. 110–249.

Gomes, D.C., Lanfredi, R.M., Pinto, R.M., de Souza, W., 1992. Description of *Trichuris travassosi* n. sp. (Nematoda: Trichurinae) from a Brazilian rodent, by light and scanning electron microscopy. Mem. Inst. Oswaldo Cruz 87, 1–10.

Hall, A., Hewitt, G., Tuffrey, V., Silva, N., 2008. A review and meta-analysis of the impact of intestinal worms on child growth and nutrition. Matern. Child Nutr. 4, 118–236.

Jenkins, T., 1969. Electron microscope observations of the body wall of *Trichuris suis*, Schrank, 1788 (Nematoda: Trichuroidea). Z. Parasitenkd. 32, 374–387.

Knoff, M., Felizardo, N.N., Iñiguez, A.M., Maldonado, A., Lopes Torres, E.J., Magalhães Pinto, R., Corrêa Gomes, D., 1890. Genetic and morphological characterisation of a new species of the genus *Hysterothylacium* (Nematoda) from *Paralichthys isosceles* Jordan, 1890 (Pisces: Teleostei) of the neotropical region, state of Rio de Janeiro, Brazil. Mem. Inst. Oswaldo Cruz 107, 186–193.

Lanfredi, R.M., Gomes, D.C., de Souza, W., 1995. Comparative study of four species of *Trichuris* Roederer, 1761 (Nematoda: Trichurinae) by scannig electron microscopy. Mem. Inst. Oswaldo Cruz 90, 489–496.

Lopes Torres, E.J., Nascimento, A.P.F., Menezes, A.O., Garcia, J., Santos, M.A.J., Maldonado Jr., A., Miranda, K., Lanfredi, R.M., de Souza, W., 2010. A new species of Trichuris from *Thrichomys apereoides* (Rodentia: Echimyidae) in Brazil: morphological and histological studies. Vet. Parasitol. 176, 226–235.

Muscariello, L., Rosso, F., Marino, G., Giordano, A., Barbarisi, M., Cafiero, G., Barbarisi, A., 2005. A critical overview of ESEM applications in the biological field. J. Cell. Physiol. 205, 328–334.

Patel, N., Kreider, T., Urban Jr., J.F., Gause, W.C., 2009. Characterization of effector mechanisms at the host: parasite interface during the immune response to tissue-dwelling intestinal nematode parasites. Int. J. Parasitol. 39, 13–21.

Robles, M.R., Navone, G.T., 2006. Redescription of *Trichuris laevitestis* (nematoda: trichuridae) from *Akodon azarae* and *Scapteromys aquaticus* (sigmodontinae: cricetidae) in Buenos Aires province, Argentina. J. Parasitol. 92, 1053–1057.

Shah, J.S., Beckett, A., 1979. A preliminary evaluation of moist environment ambient temperature scanning electron microscopy (MEATSEM). Micron 10, 13–23.

Sheffield, H.G., 1963. Electron microscopy of the bacillary band and stichosome of *Trichuris muris* and *T. vulpis*. J. Parasitol. 49, 998–1009.

Tenora, F.M., Kamiya, M., Spakulova, M., Asakava, M., Stanek, H.K.O., 1993. Scanning electron microscopy of *Trichuris suis* and *Trichuris vulpis* from Slovakia and Japan. Helminthologia 30, 93–98.

Tilney, L.G., Connelly, P.S., Guild, G.M., Vranich, K.A., Artis, D., 2005. Adaptation of a nematode parasite to living within the mammalian epithelium. J. Exp. Zool. A 303, 927–945.

Wright, K.A., 1968. Structure of the bacillary band of *Trichuris myocastoris*. J. Parasitol. 54, 1106–1110.

Wright, K.A., 1975. Cuticular inflations in whipworms *Trichuris* spp. Int. J. Parasitol. 5, 461–463.

Wright, K.A., Chan, J., 1973. Sense receptors in the bacillary band of trichuroid nematodes. Tissue Cell 5, 373–380.

Zaman, V., 1984. Scanning electron microscopy of *Trichuris trichiura* (Nematoda). Acta Trop. 41, 287–292.